Title

Targeting Gli transcription activation by small molecule suppresses tumor growth.

Journal

Oncogene, 33(16)

Authors

Bosco-Clément, G
Zhang, F
Chen, Z
et al.

Publication Date

2014-04-17

DOI

10.1038/onc.2013.164

Peer reviewed

HHS Public Access

Author manuscript

Oncogene. Author manuscript; available in PMC 2014 October 17.

Published in final edited form as:

Oncogene. 2014 April 17; 33(16): 2087–2097. doi:10.1038/onc.2013.164.

Targeting Gli Transcription Activation by Small Molecule Suppresses Tumor Growth

Geneviève Bosco-Clément[1,#], **Fang Zhang**[1,2,#], **Zhao Chen**[1,3], **Hai-Meng Zhou**[3], **Hui Li**[1], **Iwao Mikami**[1,4], **Tomomi Hirata**[1,4], **Adam Yagui-Beltran**[1], **Natalie Lui**[1], **Hanh T. Do**[1], **Tiffany Cheng**[1], **Hsin-Hui Tseng**[1], **Helen Choi**[1], **Li-Tai Fang**[1], **Il-Jin Kim**[1], **Dongsheng Yue**[1,5], **Changli Wang**[5], **Qingfeng Zheng**[1,6], **Naoaki Fujii**[7], **Michael Mann**[8], **David M. Jablons**[1,*], and **Biao He**[1,*]

[1]Thoracic Oncology Program, Department of Surgery, Helen Diller Family Comprehensive Cancer Center, University of California, San Francisco, CA 94143, USA

[2]Tsinghua University Graduate School at Shenzhen, Division of Life & Health Sciences, Shenzhen, China

[3]School of Life Sciences, Tsinghua University, Beijing 10084, China

[4]Department of Surgery, Division of Thoracic Surgery, Nippon Medical School, Tokyo 113-8602, Japan

[5]Department of Lung Cancer, Tianjin Medical University Cancer Institute & Hospital, Tianjin 300060, China

[6]Key Laboratory of Carcinogenesis and Translational Research (Ministry of Education), Thoracic Surgery II, Peking University Cancer Hospital & Institute, Beijing 100142, China

[7]Department of Chemical Biology and Therapeutics, St. Jude Children's Research Hospital, Memphis, TN, USA

[8]Division of Cardiothoracic Surgery, Department of Surgery, University of California, San Francisco, CA 94143, USA

Abstract

Targeted inhibition of Hedgehog signaling at the cell membrane has been associated with anti-cancer activity in preclinical and early clinical studies. Hedgehog signaling involves activation of Gli transcription factors that can also be induced by alternative pathways. In this study we identified an interaction between Gli proteins and a transcription co-activator TAF9, and validated its functional relevance in regulating Gli transactivation. We also describe a novel, synthetic small molecule, FN1-8, that efficiently interferes with Gli/TAF9 interaction and down-regulate Gli/

*Correspondence should be addressed to: Biao He, PhD (biao.he@ucsfmedctr.org) or David M. Jablons, MD (david.jablons@ucsfmedctr.org) Thoracic Oncology Program, Department of Surgery, Helen Diller Family Comprehensive Cancer Center, University of California San Francisco, California 94115, USA.

#These authors contributed equally

Conflict of interest: BH, MM, and DMJ have an ownership interest in Rescue Therapeutics. Other authors declare no conflict of interests.

TAF9 dependent transcriptional activity. More importantly, FN1-8 suppresses cancer cell proliferation in vitro and inhibits tumor growth in vivo. Our results suggest that blocking Gli transactivation, a key control point of multiple oncogenic pathways, may be an effective anti-cancer strategy.

Keywords

Cancer; Targeted therapy; Gli; TAF9; Hedgehog pathway

Introduction

The Hedgehog (Hh) signaling pathway controls multiple fundamental cellular functions, including cell growth and survival, cell fate determination, body patterning and organ morphogenesis (1-4). Aberrant Hh pathway activation has been implicated in a variety of inherited and sporadic malignancies (2). In the quiescent state, the twelve-pass trans-membrane Hh receptor Patched-1 (Ptch1) inhibits the activity of the seven-pass trans-membrane Hh receptor Smoothened (Smo). Binding of Hh ligands to Ptch1 reverses the inhibitory effect on Smo. Activated Smo elicits a complex series of cytoplasmic signal transduction events resulting in activation of the Glioma-associated oncogene (Gli) family of zinc-finger transcription factors (3). Target genes of Gli dependent transcription include Gli1, Ptch1, cyclin D1 and Wnt (4-7).

The importance of Hh signaling in cancer development has driven a search for modulators of this pathway, most of which to date has focused on inhibition of Hh signaling at the level of cell membrane receptors such as Smo (8,9), a key area of focus. Cyclopamine, a natural plant alkaloid that, along with its derivatives, antagonizes Smo, for example, has been used widely to inhibit the Hh pathway, and has demonstrated tumor inhibition in both in vitro and in vivo models (10-14). More recently, Smo inhibitors, such as GDC-0449, have been reported to have acceptable safety profiles and promising clinical anti-cancer activities in basal-cell carcinoma (BCC) and medulloblastoma (15-17), strongly suggesting potential clinical application in the treatment of multiple cancers through the possible suppression of cancer stem cells. Interestingly, a specific mutation in the Smo gene was recently found to confer resistance to GDC-0449 in medulloblastoma (18,19). These Smo inhibitors are currently being tested in Phase I and II clinical trials against different cancer types (20).

Increased downstream Hh pathway activation, however, has also been documented in tumors, and has been attributed to molecular mechanisms including loss of suppressor of fused (Sufu), Gli gene amplification, and chromosomal translocation (2,6,8,9). Moreover, emerging evidence has revealed additional mechanisms of Gli activation which are independent of Hh/Smo regulation, and are stimulated by the cross-talk between components downstream of Hh/Smo and several other oncogenic signaling pathways, such as the transforming growth factor β (TGFβ), epidermal growth factor receptor (EGFR), RAS and AKT/PI3K pathways (21-30). These findings suggest that Gli proteins may represent important cancer therapeutic targets. Furthermore, a recent report showed that small-molecule antagonists of Gli-mediated transcription inhibit prostate cancer cells in vitro and

in vivo (31). In this study, we identified an interaction between Gli and TBP-Associated Factor 9 (TAF9), and validated the biological relevance of this interaction in regulating Gli activity. We also designed a small-molecule inhibitor that interferes with the Gli/TAF9 interaction, and down-regulates Gli/TAF9-dependent transcription activity in cell-based assays. This compound also inhibits cancer cell proliferation in vitro and suppresses tumor growth in a xenograft model.

Results

Gli1 and Gli2 interact with TAF9 via their conserved transcription activation domain

A transcription activation domain of Gli has been identified previously at the carboxy-terminus with an acidic α-helix containing six aspartate or glutamate residues, highly similar to the herpes simplex viral protein 16 (VP16) transcription activation domain (32). The α-helical region includes the conserved motif "FXXΦΦ" (F= phenylalanine; X= any residue; Φ= any hydrophobic residue), and has been described as a putative recognition element for a transcription co-activator TAF9 (32-34). To examine whether Gli1 and Gli2 directly interact with TAF9 via their putative TAF9-binding motifs, we first performed an ELISA assay using purified recombinant His-tagged $TAF9_{1-140}$, a truncated 140-amino acid active TAF9 peptide (35) (Supplementary Figure S1a), and biotinylated Gli1 and Gli2 peptides containing the putative TAF9 binding motifs (Supplementary Table S1). Biotinylated p53 peptide containing the TAF9 binding motif has been shown to bind TAF9 and was used as a positive control (33) (Supplementary Table S1 & Figure S1b). We found that $TAF9_{1-140}$ bound to both Gli1 and Gli2 peptides in a dose dependent manner (Figure 1a). No binding signal was detected, however, when an unrelated protein control His-Fiber (36) was applied. Moreover, a mutated "FXXΦΦ" motif abolished the binding between Gli peptides and $TAF9_{1-140}$ (Figure 1a). These results suggest that Gli proteins may specifically interact with TAF9 protein through their conserved "FXXΦΦ" motif. We next validated the Gli/TAF9 binding by immunoprecipitating endogenous TAF9 in 293T cells transfected with Gli1 or Gli2 cDNA. Over-expressed Gli1 and Gli2, as well as endogenous Gli1 were readily observed in the TAF9 co-immunoprecipitates (Figure 1b). In addition, we used an in vitro transcription/translation system to translate Gli2 and c-myc tagged TAF9 proteins, and incubated them together with biotinylated oligos containing 5× wild type Gli-binding sites or 5× mutant Gli-binding sites. Then the complex was pulled down by using anti-c-myc antibody and spotted onto nylon membrane. The biotinylated oligos were then examined by using HRP-conjugated streptavidin. The results showed that the TAF9 protein, through direct binding to Gli2, was able to pull down the wild type Gli-binding sites oligos, but not the mutant ones (Figure 1c), suggesting the possible importance of Gli/TAF9 binding in Gli-dependent transcription.

To test the functional significance of Gli and TAF9 binding in human cancer cells, we investigated the effect of co-transfection of Gli and TAF9 (confirmed by RT-PCR, data not shown) on Gli-dependent transcription activity and cell proliferation. Co-expression of TAF9 with either Gli1 or Gli2 in non-small cell lung cancer (NSCLC) cell line A549 resulted in significantly higher levels of transcription of a Gli-driven luciferase construct (Gli-Luc) than those induced by Gli1 or Gli2 overexpression alone ($p< 0.001$; Figure 1d).

On the other hand, knockdown of TAF9 expression by shRNA (confirmed by RT-PCR, data not shown) in those Gli/TAF9 co-transfected A549 cells significantly down-regulated the Gli1/TAF9 or Gli2/TAF9 induced Gli-dependent transcription activity ($p< 0.001$; Supplementary Figure S1c). The proliferation rate of A549 cells was also significantly increased by Gli transfection alone and further increased by Gli/TAF9 co-transfection ($p<0.05$; Figure 1e).

A small molecule designed to interfere with the Gli/TAF9 interaction

We designed a synthetic small molecule known as FN1-8 (Figure 2a) that mimics the α-helical "FXXΦΦ" motif of Gli proteins (37). We first confirmed that FN1-8 (15 uM) significantly interferes with direct binding of TAF9 to both Gli and Gli2 proteins using ELISA ($p<0.05$; Figure 2b) and co-immunoprecipitation (Figure 2c). To examine whether FN1-8 reduces TAF9/Gli transcription activity, we treated Gli-Luc-transfected A549 cells transfected either with Gli alone or with TAF9 and Gli for 24 hours with 15 μM FN1-8. We observed that the Gli-mediated transcription activity induced either by Gli1/Gli2 alone or by Gli/TAF9 was significantly inhibited by FN1-8 (Figure 2d). While the transcription activity of Gli alone was reduced by approximately 30%, transcription activity resulting from co-transfection with TAF9 was reduced by about 50% for Gli2 and by about 70% for Gli1. We also investigated the effect of FN1-8 on the subcellular co-localization of the TAF9 and Gli proteins in cancer cells by immunofluorescent (IF) staining (Figures 2e and 2f). In control A549 cells we observed predominant co-localization of both Gli1 and Gli2 with TAF9 within the nucleus, especially around the nuclear membrane, most likely associated with transcription complexes (38-40). In FN1-8-treated A549 cells, however, this co-localization pattern was disrupted, with dissociation of both Gli1 and Gli2 from the TAF9, consistent with our IP and ELISA results.

To assess possible non-specific effects of FN1-8, we examined binding of TAF9 and the subcellular co-localization with p53 by ELISA and IF staining, respectively. We found that FN1-8 did not interfere with either binding of TAF9 or its co-localization with p53 (Figures 3a and 3b). We also examined p53-dependent transcription activity by measuring 12-repeat p53 binding site-luciferase reporter activity. After 24-hour treatment at 20 μM, FN1-8 had no effect on p53-driven luciferase expression (Figure 3c). TAF9 has been shown to bind to the terminal region of p53, stabilizing p53 and preventing the inhibitory binding of MDM2 to the same domain (33). We therefore examined p53 protein levels and the functional status of its binding protein MDM2 (phosphorylation form) after FN1-8 treatment. No noticeable effect was observed at 20 μM FN1-8 compared to the DMSO control (Figure 3d). In addition, FN1-8 did not affect the activities of several other transcription factors that we examined, such as Hypoxia inducible factor (HIF), cyclic AMP response element (CRE)-binding protein (CREB), and STAT3 (Supplementary Figure S2). Together these results suggest that FN1-8 specifically interferes with a functional Gli/TAF9 interaction.

FN1-8 inhibits the proliferation of lung cancer cells in vitro

We observed a higher level of Gli1 and Gli2 gene expression in NSCLC tissue samples compared to that in normal adult lung tissue (Figure 4a). Of 63 NSCLC samples examined, 84.1% showed over-expression of Gli1, 81.0% showed over-expression of Gli2, and 92.1%

had over-expression of at least one of the two Gli genes. Immunohistochemistry (IHC) staining of these Gli1/2 expressing NSCLC tissue specimens revealed strong nuclear localization of Gli1 and Gli2 proteins (Figure 4b). Consistently, 8 of the 10 NSCLC cell lines also over-expressed at least one of the two Gli genes (Figure 4c). These data support the relevance Gli function as a therapeutic target for NSCLC. We next treated these Gli-expressing NSCLC cell lines with FN1-8 and found that the compound inhibited the proliferation of NSCLC cells in a dose dependent manner (Figure 5a). We also observed down-regulation of endogenous Gli-regulated genes, including Ptch1 and Gli1 itself, in these FN1-8 treated cells (Figure 5b). As a test of specificity of FN1-8 and its inhibitory mechanism, we examined whether over-expressing Gli and TAF9 proteins could attenuate the growth suppression effect of FN1-8 (Figure 5c). After treatment of transfected A549 cells with 10 μM FN1-8 for 4-5 days, we noted that over-expression of either Gli2 or TAF9 alone rendered A549 cells more resistant to FN1-8 treatment than empty vector control (reduction of viable cell number: 38.9% and 41.3% vs 50.6%, respectively). Co-expressing Gli2 and TAF9 made A549 cells even more resistant than expression of either gene alone (reduction of viable cell number: 30.5%). These data again suggest that FN1-8 inhibits NSCLC cell growth via interference with the Gli/TAF9 interaction. Moreover, using a 3D-spheroid model to mimic an *in vivo* microenvironment, we observed that FN1-8-treated NSCLC cells formed smaller spheroids ($p<0.05$) (Figure 5d). The invasive phenotype of H1299 spheroids, reflected in multiple cellular branch-like structures mimicking the disruption of basal membrane, was also significantly suppressed by FN1-8 treatment ($p<0.02$) (Figure 5d). A BrdU incorporation assay showed that FN1-8 suppresses NSCLC spheroid proliferation (Figure 5e). In contrast, FN1-8 did not affect the proliferation of several normal cells that we tested (Supplementary Figure S3).

To further examine the specificity of FN1-8 towards endogenous Gli function in cancer, we compared global gene expressions in NSCLC H1299 cells after treatment with FN1-8, Gli siRNAs or cyclopamine (Figure 6). We found significant correlations in changes of global gene expressions between FN1-8 and Gli siRNA treated cells (Figure 6a, r=0.703433), cyclopamine and Gli siRNA treated cells (Figure 6b, r=0.648474), as well as FN1-8 and cyclopamine treated cells (Figure 6c, r=0.946167), respectively. Downregulation of several key effectors of the Hh/Gli pathway in the H1299 cells treated with FN1-8, Gli siRNAs or cyclopamine was also validated by real-time RT-PCR (Figure 6d). Thus, these data support that FN1-8 is specific in inhibition of endogenous Gli function in cancer.

FN1-8 inhibits non-canonical Gli activation and acts downstream of the canonical Hh pathway

Our results indicated that FN1-8 directly inhibits Gli function; we therefore hypothesized that FN1-8 suppresses Gli-dependent transcription activated by alternative pathways other than the canonical Hh signaling. To test this hypothesis, we stimulated lung cancer A549 cells with recombinant TGFβ protein (Figure 7a). We found that Gli-dependent transcription activity was significantly increased by TGFβ and that it was downregulated by FN1-8 (10 μM) to a level comparable to that without TGFβ stimulation. TGFβ-induced Gli activation, on the other hand, was not affected by treatment with cyclopamine (10 μM), a Smo inhibitor that acts on the canonical Hh signaling (11) (Figure 7a). To further examine the inhibitory

mechanism of FN1-8, we sought to determine how the upstream signaling of the canonical Hh pathway affected FN1-8. We found that FN1-8 was significantly more effective in suppressing proliferation of a pancreatic cell line BXPC3 that lacked the Smo expression (41) than in another pancreatic cell line, CFPAC, that possesses mutant Smo and intact upstream Shh signaling (41) (Figure 7b). In contrast, cyclopamine had an opposite effect in these two cell lines (Figure 7b). In another set of experiments, we found that FN1-8 was significantly more effective than cyclopamine in suppressing proliferation of a melanoma cell line LOX that lacked the Shh expression (data not shown) (Figure 7c). Addition of recombinant Shh protein into the treatments of LOX cells resulted in partial rescue of the FN1-8 treated cells (Figure 7c). Taken together, these results support that FN1-8 acts at the Gli level downstream of the canonical Hh signaling.

FN1-8 inhibits tumor growth in vivo

To verify the effect of FN1-8 in lung cancer xenografts, we first performed a pharmacokinetic (PK) study in nude mice (Supplementary Figure S4a) and confirmed the availability of FN1-8 in those animals. To examine the efficacy of FN1-8, H460 and A549 lung cancer cells were injected subcutaneously into nude mice that were treated either with vehicle control or with FN1-8 (50 mg/kg) for 12 days. FN1-8 significantly inhibited the growth of both H460 and A549-derived tumors (Figure 8a, $p=0.020$ for H460 and $p=0.024$ for A549) (Figure 8b, $p=0.036$ for H460 and $p=0.045$ for A549). No obvious changes in the body weights of FN1-8 treated mice were observed during the treatment course (Supplementary Figure S4b). At the completion of the experiment, we analyzed the effect of FN1-8 on Gli function in the tumors dissected from those xenografts. We found that FN1-8 significantly reduced mRNA expression of Ptch1 and Gli1 in both H460 and A549-derived tumors (Figure 8c). No noticeable toxicity was observed in organs from FN1-8-treated mice, and leukocyte populations in those mice were also in the normal ranges (Supplementary Figures S4c and S4d).

Discussion

Abnormal activation of the Hh pathway in cancer may occur through different mechanisms (2): constitutive activation through loss- or gain-of function mutations of the pathway receptors (mutation-driven activation), autocrine activation in the same tumor cell or adjacent ones, and paracrine activation involving the tumor-adjacent stroma (ligand-driven activation). Although final effectors of canonical Hh signaling regardless of its activation mechanism, the Gli family of transcription factors can also be activated by other oncogenic pathways independent of the Hh/Smo regulation (21-30). The complexity of Gli activation suggests that Gli may be a key control point for cross-talk among these oncogenic pathways in cancer, and that Gli is a good target for the development of cancer therapeutics.

Indeed, several recent efforts have been made to identify Gli-mediated transcriptional inhibitors. Inhibitors (31,42-45) have been identified primarily through cell-based screening assay systems that contain a Gli-dependent luciferase reporter. In this study we report the identification and validation of the interaction between Gli and TAF9 as a putative therapeutic target, as well as the design of an inhibitor of the Gli/TAF9 interaction that

suppresses tumor cell growth in vitro and in vivo. TAF9 has been shown to be a major component of the general transcription factor complex TFIID (38-40). A conserved motif "FXXΦΦ" has been identified previously within the transcription activation domain of the Gli proteins and has been described as a putative recognition element for TAF9 (32-34). The data presented here, however, are the first direct evidence of an interaction between Gli and TAF9. We demonstrated several ways that TAF9 interacts directly with both Gli1 and Gli2 though the conserved "TAF9-binding" motif. As a control, a mutation in this motif abolished Gli-TAF9 binding. Nuclear co-localization of both Gli1 and Gli2 with TAF9 protein was also observed. More importantly, the Gli/TAF9 interaction appeared to be functionally important for Gli-mediated transcriptional activity and for cancer cell proliferation. Taken together, these data suggest that Gli1 and Gli2 directly interact with TAF9 in a Gli-dependent transcriptional machinery that is important for cancer cells.

Small molecules targeting the protein-protein interactions of transcription factors have recently been reported as promising cancer therapeutics (46-48). In order to target the Gli/TAF9 interaction, we modeled the 3D structure of the conserved motif "FXXΦΦ" of Gli proteins and observed an α-helix structure (37), consistent with the previous report (32). Rational chemical design was then employed to design small molecule compounds comprising a pyrazoline structure to mimic the structure of this motif (37). In this study, we showed that one of those compounds, FN1-8, was able to specifically disrupt the Gli1/TAF9 and Gli2/TAF9 interactions, and to reduce Gli-mediated transcriptional activity. Interestingly, FN1-8 disrupted co-localization of both Gli1 and Gli2 with TAF9 within the nucleus of cancer cells, suggesting that binding to TAF9 within the transcriptional complex may be important for Gli1 and Gli2 nuclear localization. Because TAF9 has been shown to bind to the terminal region of p53 and stabilize p53 function (33), we examined whether FN1-8 interferes with the p53/TAF9 interaction and p53 function as a specificity control. We found that FN1-8 did not interfere with the binding of and co-localization between TAF9 and p53, or with p53-dependent transcription activity. The p53-TAF9 binding motif may therefore have a 3D conformation different from that of the Gli proteins; alternatively, the binding affinity between TAF9 and p53 may be higher than that between TAF9 and Gli. Together with our results that transcriptional activity of several other transcription factors was not affected by FN1-8 treatment, it seems that FN1-8 is a relatively specific antagonist for the functional Gli/TAF9 interaction.

In addition to our observation that FN1-8 significantly suppresses canonical Hh/Gli target gene expression as well as the proliferation of lung cancer cells in vitro and in vivo, we also demonstrated that FN1-8 suppresses TGFβ-induced Gli activation and inhibits cancer cell proliferation without upstream canonical Hh/Smo signaling in vitro. In contrast, cyclopamine, a Smo inhibitor, had no effect on non-canonical Gli activation and was less potent in growth inhibition of cancer cells lacking upstream canonical Hh/Smo signaling. These data support our hypothesis that Gli function may be a better therapeutic target because of its putative critical role as a control point for multiple oncogenic pathways in cancer. Furthermore, FN1-8 was found to inhibit proliferation of a number of disparate cancer cells that expressed Gli proteins other than lung cancer, including prostate cancer, pancreatic cancer, colon cancer and glioma (data not shown), consistent with previous reports of downstream activation of Hh pathway effectors in those cancer types (8-14). Our

results indicate that targeting Gli function may have broader implications for the clinical development of Hh pathway inhibitors in cancer treatment.

Materials and Methods

Cell lines and tissue samples

Most human cell lines (lung cancer A549, A427, H1299, H460, H322, H838, H1703, and H522; colon cancer SW480, HCT116, and HT29; melanoma LOX; human normal skin fibroblast, muscle cells, renal cell line HRE152, 293T) were obtained from the American Type Culture Collection (ATCC). Human pancreatic cancer cell lines BxPC3 and CFPAC-1 were kindly provided by Dr. Hebrok at the UCSF. Stable cell lines: NF-kB-luciferase reporter in A549, HIF-luciferase reporter in NIH3T3, and CREB-luciferase reporter in 293T were purchased from Panomics. Cell lines were cultured in RPMI 1640 or DMEM supplemented with 10% fetal bovine serum at 37°C in a humid incubator with 5% CO_2. Fresh NSCLC and normal tissue samples from patients undergoing resection of their tumors were collected at the time of surgery (IRB approval H8714-15319-040) at UCSF, and immediately snap-frozen in liquid nitrogen and were kept at −170°C in a liquid nitrogen freezer until further use.

Plasmids, transfection and luciferase assays

Human $TAF9_{1-140}$ cDNA was a gift from Dr. Quackenbush at Colorado State University. Human Gli1 cDNA was kindly provided by Dr. Vogelstein at the Johns Hopkins University. Human Gli2 cDNA was kindly provided by Dr. Aberger at University of Salzburg, Austria. 8×Gli binding sites-luciferase reporter and its matched control, mutant Gli binding sites-luciferase reporter were kindly provided by Dr. Hebrok at the UCSF. TOPFLASH/FOPFLASH reporters were purchased from Upstate. TAF9 (cat# KH09657) and negative control shRNAs were purchased from SABiosciences. Transfections and luciferase assays were performed as we previously described (49,50).

RNA extraction and RT-PCR

Total RNA of cell lines or tissues was extracted using TRIzol LS (Invitrogen) or Qiagen RNeasy Mini Kit. For quantitative Real-time RT-PCR, cDNA synthesis and Taqman PCR were performed as previously described (51). Hybridization probes and primers were purchased from Applied Biosystems (ABI). For semi-quantitative RT-PCR, One-step RT-PCR Kit (Invitrogen) was used and primers were purchased from Operon. Primer sequences are in Supplementary Table S1.

Enzyme-linked immunosorbent assay

Biotinylated TAF9 binding motifs of Gli1 and Gli2 proteins, mutant GLI2-TAF9bd and p53-TAF9bd (33) were custom synthesized (Genemed Synthesis). Sequences of these peptides are in Supplementary Table S2. Recombinant His-$hTAF9_{1-140}$ protein was obtained by expressing the $TAF9_{1-140}$/pET19b plasmid in BL21 cells and purified as previously described (35). Recombinant His-tagged viral membrane protein His-Fiber (kindly provided by Dr. McCormick at UCSF) was used as a negative control. Biotin-peptides were resuspended in 50%DMSO/50%PBS at 1ug/ul, and diluted in Binding Buffer (TBS/

0.1%BSA/0.05%Tween-20) at the final concentration as indicated. Peptides were immobilized on the Reacti-bind ™ Streptavidin High Binding Capacity coated plates (PIERCE) overnight at 4°C. Recombinant His-proteins was diluted in Binding Buffer at 2∼5ug/ml. Compounds were added to His-protein/Binding buffer at the indicated concentrations, followed by incubation with the immobilized peptides on plates. After washing, plates were incubated with anti-His mouse mAb (27E8) and followed by AP-conjugated anti-mouse IgG (Cell Signaling; 1:1000) before adding 100ul/well of the Alkaline Phosphatase Substrate (BioRad). Signal was detected by using a Microplate Reader (BioTek).

Co-immunoprecipitation and immunoblotting

293T cells transfected with Gli1 or Gli2 were harvested after 24 hours post-transfection treatments of compounds (20 uM) or DMSO for 5-6 hours. Cells were then lysed on ice in NP40 Lysis Buffer supplemented with protease inhibitors cocktail (Sigma), and 1000-1500 μg of total protein lysate was used for co-IP. Endogenous TAF9 was immunoprecipitated with anti-TAF9 anitbody (N-16, Santa Cruz) and subsequent immunoblotting was performed with antibodies: Gli1 or Gli2 (Cell Signaling), TAF9 (N-16, Santa Cruz), and p53 (DO-1, Calbiochem). Other Western blots were performed as previously described (Okamoto et al., 2010). Primary antibodies used include: p-MDM2 and c-myc (Cell Signaling); p53 and β-actin (Sigma).

Immunofluorescent staining

Cells seeded in 2-chamber TC slides (Lab-Tek) were subjected to different treatments before fixed with MeOH:Acetone (1:1) for 10min at -20°C. Cells were permeablized with 0.5%TritonX-100/PBS for 2min and blocked in 10%FBS/PBS for 1hr at RT, followed by overnight incubation with primary antibodies (Gli1 and Gli2 (ab49314 and ab26056, Abcam); p53 (DO-1, Calbiochem); TAF9 (N-16, Santa Cruz)) at 4°C. After washing with PBS, cells were incubated with secondary Alexa488-conjugated IgG for 1hr at RT. For BrdU staining, an anti-BrdU Alexa488-conjugated mouse antibody was used for incubation at 4°C. Slides were mounted in VectorShield mounting media with DAPI (Vector), and images were acquired with Zeiss LSM510 META confocal microscope.

Immunohistochemistry staining

Performed as previously described (52). Dilution used for staining was 1:100 and 1:200 for anti-Gli1 and anti-Gli2 antibodies, respectively.

Compounds

FN1-8 was synthesized and analyzed by liquid chromatography mass spectrometry as we previously described (37). Cyclopamine and tomatidine were purchased from Sigma. All compounds were dissolved in DMSO at 30mM as stocks and stored at -20°C before further uses.

Proliferation assay and three-dimension (3D) culture

Performed as previously described (50).

Microarray analysis

NSCLC cell line H1299 was treated with 10μM FN1-8 or 10μM cyclopamine for 48 hours. For siRNA treatment, cells were transfected simultaneously with Gli1 and Gli2 siRNAs (total 5ng) for 72 hours. Total RNA of the treated cells was then extracted using Qiagen RNeasy Mini Kit. 250 ng of total RNA was amplified into cRNA and made into cDNA using the Ambion WT Expression Kit. 5.5 ug of the cDNA was then fragmented using the Affymetrix GeneChip WT Terminal Labeling kit and confirmed by running on the Agilent Bioanalyzer using the RNA 6000 kit. The fragmented cDNA was labeled using the Affymetrix GeneChip WT Terminal Labeling kit and added into the hybridization cocktail that was prepared according to the protocol included in the Affymetrix GeneTitan Hybridization Wash and Stain kit. The samples were finally loaded into the Affymetrix GeneTitan MC at the UCSF Thoracic Oncology Laboratory for hybridization, washing, and scanning. Raw signal intensities were extracted with Agilent Feature Extraction software. mRNA expression profiles from compounds and siRNAs treated cells were compared with control cells to get gene expression changes. The expression changes by FN1-8, cyclopamine, and Gli siRNAs were compared in pairs to evaluate the correlation.

in vivo studies

All experiments were performed at the UCSF Preclinical Core in accordance with UCSF institutional guidelines. For pharmacokinetic study, mice (3/group) were i.p. injected in the abdomens with compound FN1-8 (30mg/kg body weight). Then plasma was collected from the tail-vein of each mouse at 10 min, 2 hours, 6 hours and 24 hours after injection. The FN1-8 concentration in each plasma sample was determined by mass spec. For efficacy study, ten mice (female athymic nude mice NCRNU-M (Taconic)) were used in each group and injected s.c. with 3×10^6/100μl human cancer cells in the dorsal area. Tumors were allowed to grow for 7 days after inoculation to become visible nodules. Animals were then i.p. injected with compound FN1-8 (50mg/kg body weight) or vehicle control daily around the same time for 12 days. Tumors were allowed to grow for an additional week after completion of the treatments. Tumor size was measured and tumor volumes were calculated using width (x) and length (y) ($x^2y/2$, where $x < y$). For toxicity analysis, body weights of the treated mice were monitored throughout the dosing period. Organs were also resected from mice at completion of the efficacy study. The specimens were fixed in 4% buffered formaldehyde, embedded in paraffin, sectioned, and histologically analyzed by hematoxylin and eosin (HE) staining. The HE stained slides were then examined by a mouse pathologist for toxicity evidence. Additionally, leukocytes from each animal were collected and leukocyte population was counted through a blood cell counter. Data was presented as mean values (± S.D.).

Statistical analysis

All data were calculated as means ± standard deviations. Differences between groups were compared with a two-sided student's t-test. A *p* value of 0.05 or less was considered to be significant.

Supplementary Material

Refer to Web version on PubMed Central for supplementary material.

Acknowledgments

This work was supported by Joan's Legacy: Uniting Against Lung Cancer Research Grant, NIH/NCI grant R01CA125030, and the Eileen D. Ludwig Endowed for Thoracic Oncology Research (to BH); NIH/NCI grant R01CA132566, the Bonnie J. Addario Lung Cancer Foundation, the Kazan, McClain, Abrams, Fernandez, Lyons, Greenwood, Harley & Oberman Foundation, Honeywell Foundation, and the Barbara Isackson Lung Cancer Research Fund (to DMJ).

References

1. Varjosalo M, Taipale J. Hedgehog: functions and mechanisms. Genes Dev. 2008; 22:2454–2472. [PubMed: 18794343]
2. Merchant AA, Matsui W. Targeting Hedgehog--a cancer stem cell pathway. Clin Cancer Res. 2010; 16:3130–3140. [PubMed: 20530699]
3. Kalderon D. Transducing the Hedgehog signal. Cell. 2000; 103:371–374. [PubMed: 11081624]
4. Hooper JE, Scott MP. Communicating with Hedgehogs. Nat Rev Mol Cell Biol. 2005; 6:306–317. [PubMed: 15803137]
5. Huangfu D, Anderson KV. Signaling from Smo to Ci/Gli: Hedgehog pathways from Drosophila to vertebrates. Development. 2006; 133:3–14. [PubMed: 16339192]
6. Ruiz i Altaba A, Mas C, Stecca B. The Gli code: and information nexus regulating cell fate, stemness and cancer. Trends Cell Biol. 2007; 17:438–447. [PubMed: 17845852]
7. Mullor JL, Dahmane N, Sun T, Ruiz i Altaba A. Wnt signals are targets and mediators of Gli function. Curr Biol. 2001; 1:769–773. [PubMed: 11378387]
8. Yang L, Xie G, Fan Q, Xie J. Activation of the hedgehog-signaling pathway in human cancer and the clinical implications. Oncogene. 2010; 29:469–481. [PubMed: 19935712]
9. Scales SJ, de Sauvage FJ. Mechanisms of Hedgehog pathway activation in cancer and implications for therapy. Trends Pharmacol Sci. 2009; 30:303–312. [PubMed: 19443052]
10. Berman DM, Karhadkar SS, Hallahan AR, Pritchard JI, Eberhart CG, Watkins DN, et al. Medulloblastoma growth inhibition by hedgehog pathway blockade. Science. 2002; 297:1559–1561. [PubMed: 12202832]
11. Watkins DN, Berman DM, Burkholder SG, Wang B, Beachy PA, Baylin SB. Hedgehog signalling within airway epithelial progenitors and in small-cell lung cancer. Nature. 2003; 422:313–317. [PubMed: 12629553]
12. Karhadkar SS, Bova GS, Abdallah N, Dhara S, Gardner D, Maitra A, et al. Hedgehog signalling in prostate regeneration, neoplasia and metastasis. Nature. 2004; 431:707–712. [PubMed: 15361885]
13. Feldmann G, Dhara S, Fendrich V, Bedja D, Beaty R, Mullendore M, et al. Blockade of hedgehog signaling inhibits pancreatic cancer invasion and metastases: a new paradigm for combination therapy in solid cancers. Cancer Res. 2007; 67:2187–2196. [PubMed: 17332349]
14. Clement V, Sanchez P, de Tribolet N, Radovanovic I, Ruiz i Altaba A. HEDGEHOGGLI1 signaling regulates human glioma growth, cancer stem cell self- renewal, and tumorigenicity. Curr Biol. 2007; 17:165–172. [PubMed: 17196391]
15. Rudin CM, Hann CL, Laterra J, Yauch RL, Callahan CA, Fu L, et al. Treatment of medulloblastoma with hedgehog pathway inhibitor GDC-0449. N Engl J Med. 2009; 361:1173–1178. [PubMed: 19726761]
16. LoRusso PM, Rudin CM, Reddy JC, Tibes R, Weiss GJ, Borad MJ, et al. Phase I trial of hedgehog pathway inhibitor vismodegib (GDC-0449) in patients with refractory, locally advanced or metastatic solid tumors. Clin Cancer Res. 2011; 17:2502–2511. [PubMed: 21300762]
17. Tremblay MR, Lescarbeau A, Grogan MJ, Tan E, Lin G, Austad BC, et al. Discovery of a potent and orally active Hedgehog pathway antagonist (IPI-926). J Med Chem. 2009; 52:4400–4418. [PubMed: 19522463]

18. Yauch RL, Dijkgraaf GJ, Alicke B, Januario T, Ahn CP, Holcomb T, et al. Smoothened mutation confers resistance to a Hedgehog pathway inhibitor in medulloblastoma. Science. 2009; 326:572–574. [PubMed: 19726788]
19. Dijkgraaf GJ, Alicke B, Weinmann L, Januario T, West K, Modrusan Z, et al. Small molecule inhibition of GDC-0449 refractory smoothened mutants and downstream mechanisms of drug resistance. Cancer Res. 2011; 71:435–444. [PubMed: 21123452]
20. Low JA, de Sauvage FJ. Clinical experience with Hedgehog pathway inhibitors. J Clin Oncol. 2010; 28:5321–5326. [PubMed: 21041712]
21. Dennler S, André J, Alexaki I, Li A, Magnaldo T, ten Dijke P, et al. Induction of sonic hedgehog mediators by transforming growth factor-beta: Smad3-dependent activation of Gli2 and Gli1 expression in vitro and in vivo. Cancer Res. 2007; 67:6981–6986. [PubMed: 17638910]
22. Dennler S, André J, Verrecchia F, Mauviel A. Cloning of the human Gli2 promoter: transcriptional activation by Tgf-Beta via Smad3/beta-Catenin cooperation. J Biol Chem. 2009; 284:31523–31531. [PubMed: 19797115]
23. Guo X, Wang XF. Signaling cross-talk between TGF-beta/BMP and other pathways. Cell Res. 2009; 19:71–88. [PubMed: 19002158]
24. Ji ZY, Mei FC, Xie J, Cheng X. Oncogenic KRAS activates hedgehog signaling pathway in pancreatic cancer cells. J Biol Chem. 2007; 282:14048–14055. [PubMed: 17353198]
25. Riobo NA, Haines GM, Emerson CP Jr. Protein kinase C-delta and mitogen-activated protein/extracellular signal-regulated kinase-1 control GLI activation in hedgehog signaling. Cancer Res. 2006; 66:839–845. [PubMed: 16424016]
26. Riobo NA, Lu K, Ai X, Haines GM, Emerson CP Jr. Phosphoinositide 3-kinase and Akt are essential for Sonic Hedgehog signaling. Proc Natl Acad Sci USA. 2006; 103:4505–4510. [PubMed: 16537363]
27. Schnidar H, Eberl M, Klingler S, Mangelberger D, Kasper M, Hauser-Kronberger C, et al. Epidermal growth factor receptor signaling synergizes with Hedgehog/GLI in oncogenic transformation via activation of the MEK/ERK/JUN pathway. Cancer Res. 2009; 69:1284–1292. [PubMed: 19190345]
28. Stecca B, Mas C, Clement V, Zbinden M, Correa R, Piguet V, et al. Melanomas require HEDGEHOG-GLI signaling reaulated by interactions between GLI1 and the RAS-MEK/AKT pathways. Proc Natl Acad Sci USA. 2007; 104:5895–5900. [PubMed: 17392427]
29. Pasca di Magliano M, Sekine S, Ermilov A, Ferris J, Dlugosz AA, Hebrok M. Hedgehog/Ras interactions regulate early stages of pancreatic cancer. Genes Dev. 2006; 20:3161–3173. [PubMed: 17114586]
30. Lauth M, Toftgård R. Non-canonical activation of GLI transcription factors. Cell Cycle. 2007; 6:2458–2463. [PubMed: 17726373]
31. Lauth M, Bergstrom A, Shimokawa T, Toftgård R. Inhibition of GLI-mediated transcription and tumor cell growth by small-molecule antagonists. Proc Natl Acad Sci USA. 2007; 104:8455–8460. [PubMed: 17494766]
32. Yoon JW, Liu CZ, Yang JT, Swart R, Iannaccone P, Walterhouse D. GLI activates transcription through a herpes simplex viral protein 16-like activation domain. J Biol Chem. 1998; 273:3496–3501. [PubMed: 9452474]
33. Uesugi M, Verdine GL. The alpha-helical FXXPhiPhi motif in p53: TAF interaction and discrimination by MDM2. Proc Natl Acad Sci USA. 1999; 96:14801–14806. [PubMed: 10611293]
34. Choi Y, Asada S, Uesugi M. Divergent hTAFII31-binding motifs hidden in activation domains. J Biol Chem. 2000; 275:15912–15916. [PubMed: 10821850]
35. Rovnak J, Quackenbush SL. Walleye dermal sarcoma virus retroviral cyclin directly contacts TAF9. J Virol. 2006; 80:12041–12048. [PubMed: 17035330]
36. Falgout B, Ketner G. Characterization of adenovirus particles made by deletion mutants lacking the fiber gene. J Virol. 1988; 62:622–625. [PubMed: 3275791]
37. He, B.; Fujii, N.; You, L.; Xu, Z.; Jablons, DM. Targeting Gli proteins in human cancer by small molecules. US Patent No. 7714014. 2010.
38. Ogryzko VV, Kotani T, Zhang X, Schiltz RL, Howard T, Yang XJ, et al. Histone-like TAFs within the PCAF histone acetylase complex. Cell. 1998; 94:35–44. [PubMed: 9674425]

39. Hoffmann A, Chiang CM, Oelgeschläger T, Xie X, Burley SK, Nakatani Y, et al. A histone octamer-like structure within TFIID. Nature. 1996; 380:356–359. [PubMed: 8598932]
40. Shao H, Revach M, Moshonov S, Tzuman Y, Gazit K, Albeck S, et al. Core promoter binding by histone-like TAF complexes. Mol Cell Biol. 2005; 25:206–219. [PubMed: 15601843]
41. Yauch RL, Gould SE, Scales SJ, Tang T, Tian H, Ahn CP, et al. A paracrine requirement for hedgehog signaling in cancer. Nature. 2008; 455:406–410. [PubMed: 18754008]
42. Hosoya T, Arai MA, Koyano T, Kowithayakorn T, Ishibashi M. Naturally occurring small-molecule inhibitors of hedgehog/GLI-mediated transcription. Chembiochem. 2008; 9:1082–1092. [PubMed: 18357592]
43. Hyman JM, Firestone AJ, Heine VM, Zhao Y, Ocasio CA, Han K, et al. Small- molecule inhibitors reveal multiple strategies for Hedgehog pathway blockade. Proc Natl Acad Sci USA. 2009; 106:14132–14137. [PubMed: 19666565]
44. Rifai Y, Arai M, Sadhu S, Ahmed F, Ishibashi M. New Hedgehog/GLI signaling inhibitors from Excoecaria Agallocha. Bioorganic & Medicinal Chem Lett. 2011; 21:718–722.
45. Arai M, Tateno C, Koyano T, Kowithayakorn T, Kawabe S, Ishibashi M. New hedgehog/GLI-signaling inhibitors from Adenium obesum. Org Biomol Chem. 2011; 9:1133–1139. [PubMed: 21170436]
46. Jung D, Choi Y, Uesugi M. Small organic molecules that modulate gene transcription. Drug Discov Today. 2006; 11:452–457. [PubMed: 16635809]
47. Shimogawa H, Kwon Y, Mao Q, Kawazoe Y, Choi Y, Asada S, et al. A wrench-shaped synthetic molecule that modulates a transcription factor-coactivator interaction. J Am Chem Soc. 2004; 126:3461–3471. [PubMed: 15025473]
48. Vassilev LT, Vu BT, Graves B, Carvajal D, Podlaski F, Filipovic Z, et al. In vivo activation of the p53 pathway by small-molecule antagonists of MDM2. Science. 2004; 303:844–848. [PubMed: 14704432]
49. Reguart N, He B, Xu Z, You L, Lee AY, Mazieres J, et al. Cloning and characterization of the promoter of human Wnt inhibitory factor-1. Biochem Biophys Res Commun. 2004; 323:229–234. [PubMed: 15351726]
50. Okamoto J, Hirata T, Chen Z, Zhou HM, Mikami I, Li H, et al. EMX2 is epigenetically silenced and suppresses growth in human lung cancer. Oncogene. 2010; 29:5969–5975. [PubMed: 20697358]
51. Raz D, Ray MR, Kim JY, He B, Taron M, Skrzypski M, et al. A multi-gene assay is prognostic of survival in patients with early-stage lung adenocarcinoma. Clin Cancer Res. 2008; 14:5565–5570. [PubMed: 18765549]
52. Okamoto J, Kratz JR, Hirata T, Mikami I, Raz D, Segal M, et al. Downregulation of EMX2 is associated with clinical outcomes in lung adenocarcinoma patients. Clin Lung Cancer. 2011; 12:237–244. [PubMed: 21726823]

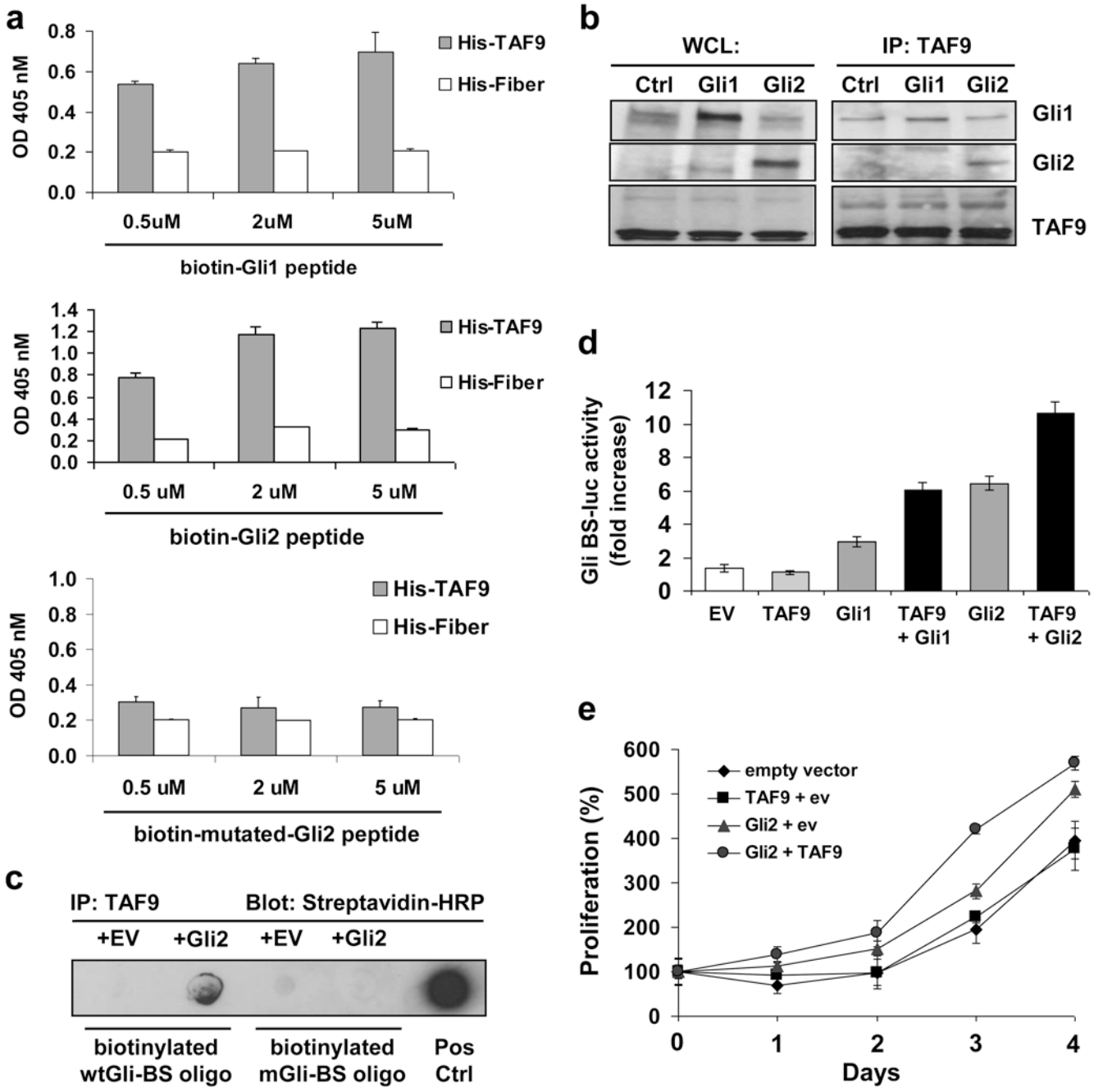

Figure 1.

Gli1 and Gli2 interact with TAF9 via their conserved transcription activation domain. (**a**) ELISA assays of biotinylated Gli1 and Gli2 peptides (with wild-type TAF9 binding motif) with purified recombinant His-hTAF9$_{1\text{-}140}$ protein. Purified recombinant His-Fiber protein was used as a negative control. Biotinylated Gli2 peptide with mutated TAF9 binding motif (wild type "FDAIM" was mutated to "ADAIA") was used as a specificity control. (**b**) 293T cells transfected with Gli1 or Gli2 cDNA was harvested and subjected to immunoprecipitation with an anti-TAF9 antibody (right panels); Left panels are Western

blotting of whole cell lysates as controls of protein input for co-IP. Precipitated TAF9 was confirmed by the TAF9 antibody. Note that endogenous Gli1 was pulled down in both the control ("Ctrl") and Gli2-transfected ("Gli2") cells. (**c**) Gli2 and TAF9 binding to DNA oligos with Gli-binding sites. Positive control (Pos Ctrl) is biotinylated DNA oligos directly spotted on the membrane. EV: empty pcDNA3.1 vector used as a negative control in the in vitro translation reactions. (**d**) Gli/TAF9-induced transcriptional activation in NSCLC cell line A549. An expression construct linking the 8 repeats of Gli-binding sites (Gli BS) to a luciferase reporter was used as a surrogate measurement of the Gli-dependent transcription. All measured luciferase activities were normalized to pRL-TK vector activity. The data represent means ± S.D. (**e**) MTS assay of A549 cells transfected with Gli2 or TAF9 cDNA. The data represent means ± S.D.

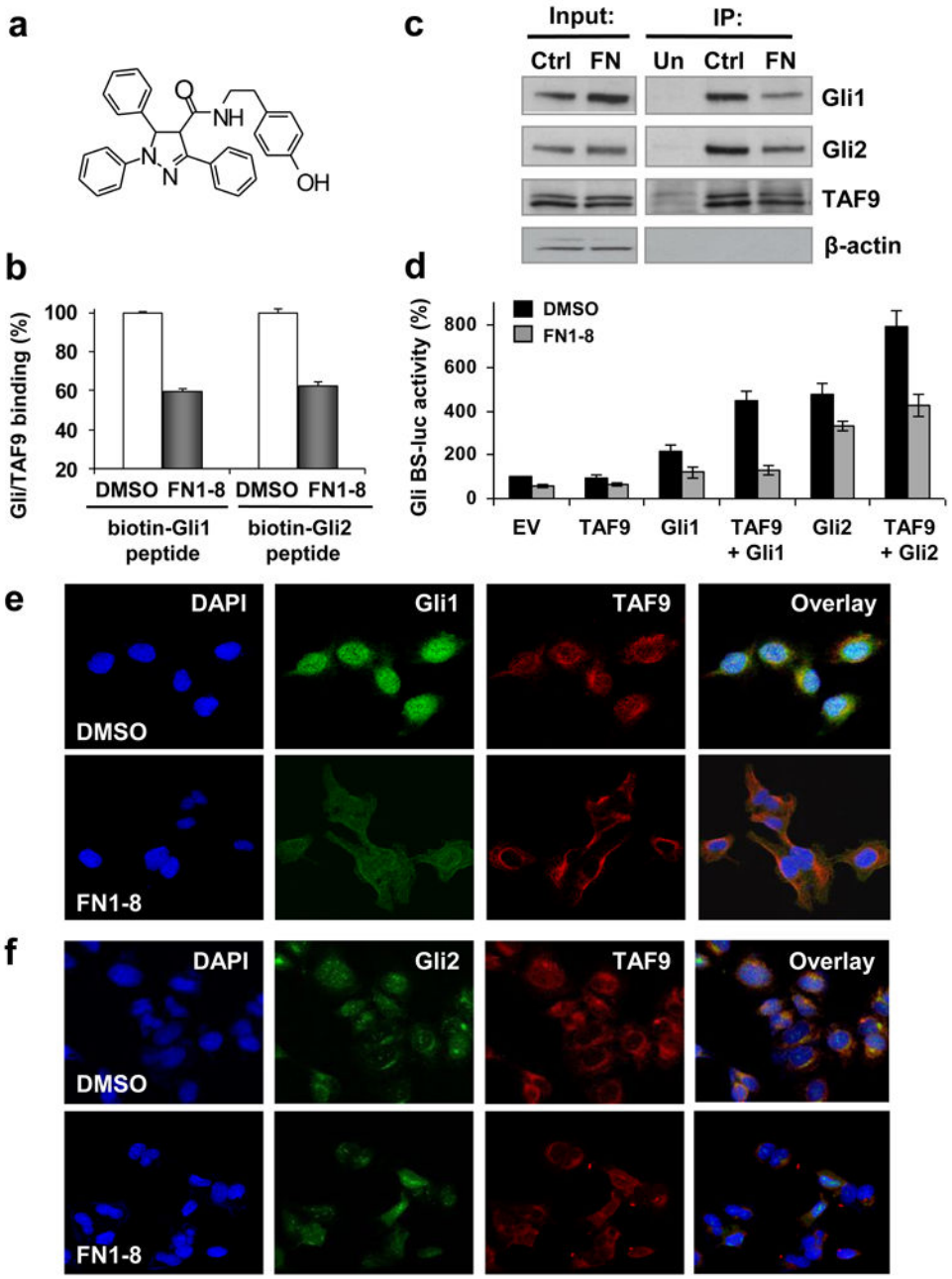

Figure 2.

Small molecule FN1-8 interferes with the Gli/TAF9 interaction. (**a**) The structure of FN1-8. (**b**) Effect of FN1-8 on Gli/TAF9 binding in ELISA assays (15μM FN1-8 was incubated with the binding reaction mix for 2 hours). (**c**) 293T cells transfected with Gli1 or Gli2 with and without FN1-8 (FN) treatment (15μM) were harvested and subjected to immunoprecipitation (IP) with an anti-TAF9 antibody (right panels); Left panels are Western blotting of whole cell lysates as controls of protein input for co-IP. 293T cells treated with DMSO and IP using TAF9 antibody (Ctrl), and IP using an unrelated antibody (Un) were included as controls. Precipitated TAF9 was also confirmed by the TAF9

antibody (bottom panel). (**d**) FN1-8 (15μM treatment for 1 day) inhibits the Gli/TAF9 dependent transcription activity in NSCLC cell line A549. All measured luciferase activities were normalized to pRL-TK vector activity. The data represent means ± S.D. (**e**) and (**f**) Immunofluorescent (IF) staining of A549 cells after FN1-8 treatment (15μM) for 2 days for TAF9 (red), Gli1 (**e**; green) and Gli2 (**f**; green). In overlay, co-localization of Gli1 or Gli2 with TAF9 becomes yellow. DAPI was used to label nucleus.

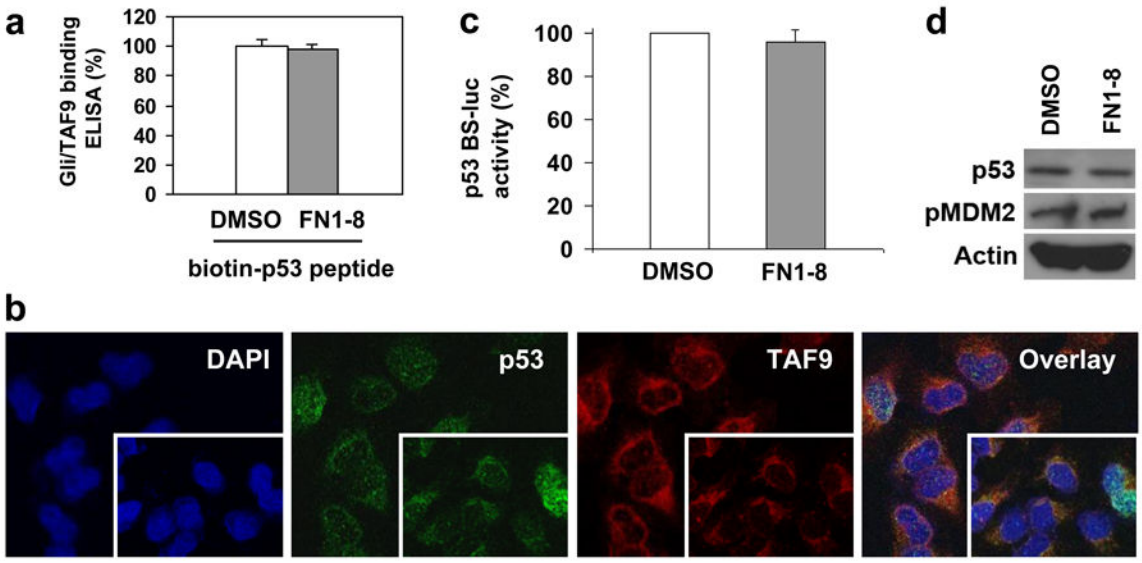

Figure 3.

Effect of FN1-8 on the p53/TAF9 interaction. (**a**) ELISA assay of the binding between TAF9 and p53 with and without FN1-8 treatment (15uM). (**b**) Immunofluorescent (IF) staining of 293T cells for TAF9 (red) and p53 (green). In overlay, co-localization of p53 with TAF9 becomes yellow. DAPI was used to label nucleus. Outside panels are DMSO control treated cells and inserts are FN1-8 treated cells (15μM for 2 days). (**c**) p53 binding sites-luciferase reporter activity in 293T cells was not affected by FN1-8 (20μM, 1 day). All measured luciferase activities were normalized to pRL-TK vector activity. The data represent means ± S.D. (**d**) Western blot of p53 and pMDM2 in 293T cells after FN1-8 treatment (20μM, 3 day). 20 μg total proteins were loaded in each lane. *β*-actin was used as a loading control.

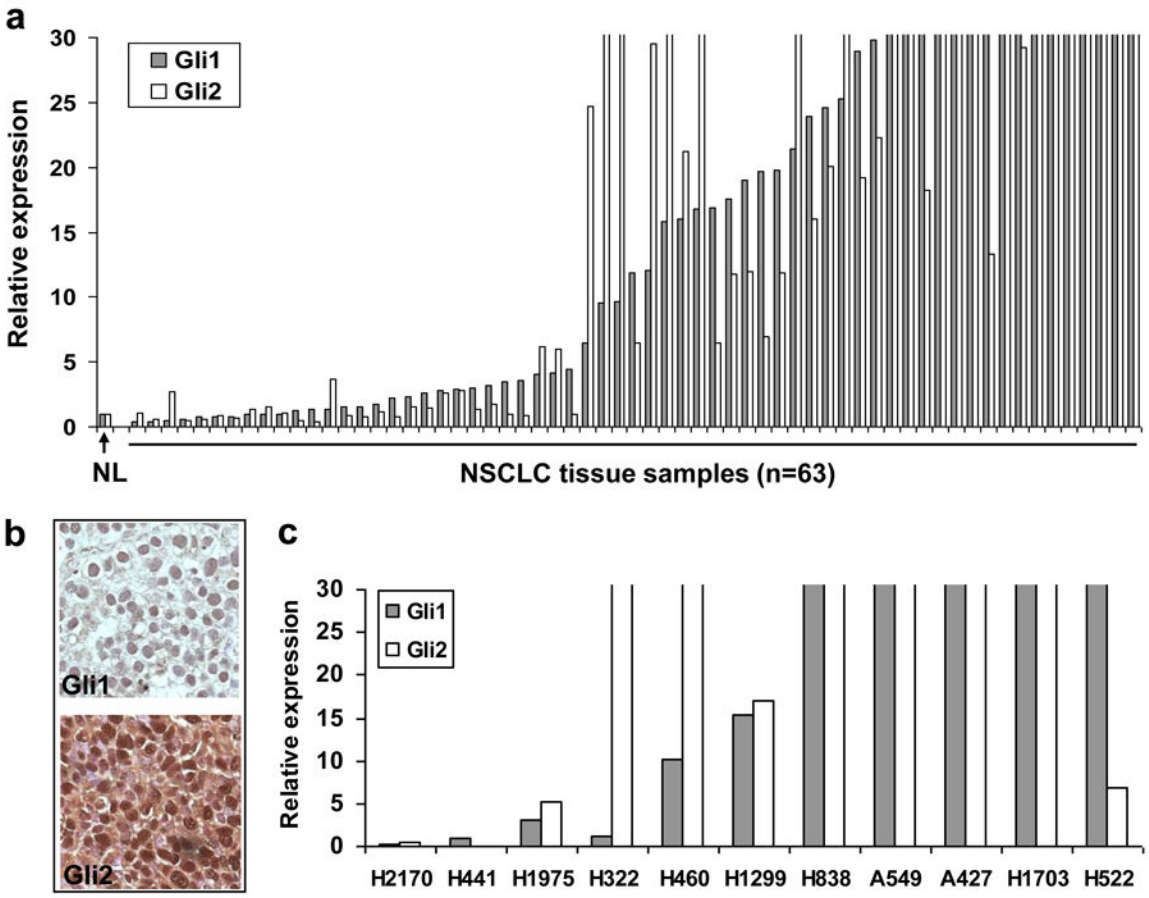

Figure 4.

Expression analysis of Gli1 and Gli2 in NSCLC. (**a**) Real-time RT-PCR in 63 fresh human NSCLC tissue samples. (**b**) IHC staining of fresh human NSCLC tissue. Dilution used for staining was 1:100 and 1:200 for anti-Gli1 and anti-Gli2 antibodies, respectively. Images were taken under a light microscope (×200). (**c**) Real-time RT-PCR analysis in NSCLC cell lines. For real-time RT-PCR, expressions in each sample were normalized to 18s rRNA and calculated by using $2^{-\text{deltaCt}}$ method, then further normalized to that of adult normal lung (NL) tissue which was set to 1. Expressions of both Gli1 and Gli2 in many samples are off the scale (y-axis).

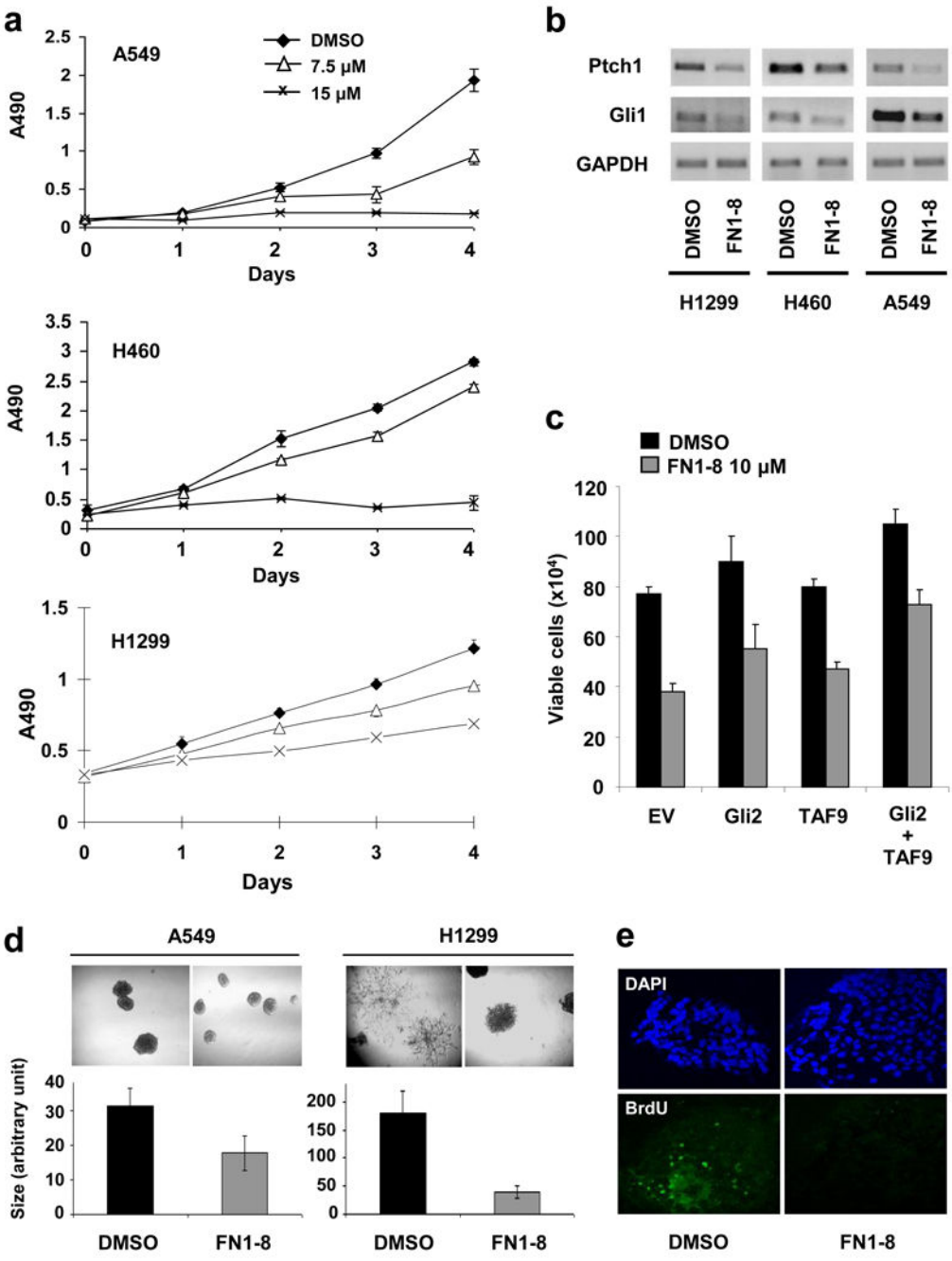

Figure 5.

Small molecule FN1-8 suppresses proliferation of lung cancer cells in vitro. (**a**) MTS assay of lung cancer cell lines treated with different doses of FN1-8. Results are mean value of triplicate ± S.D. (error bars). (**b**) Semi-quantitative RT-PCR analysis of target genes of the Gli transcription. GAPDH served as a loading control. (**c**) Forced expression of Gli2 and TAF9 rescues A549 cells treated with FN1-8. Viable cells were stained with Trypan Blue and counted after each treatment (10μM for 5 days). 0.5 μg each cDNA was used in each transfection. (**d**) Spheroid size was quantified using Image J software, and data were

representative of three independent experiments with similar results. (**e**) BrdU staining of A549 3D spheroids after FN1-8 treatment (10μM). Slides were mounted in Vector Shield mounting media with DAPI (Vector) and images were captured with Zeiss LSM510 META confocal microscope (Zeiss).

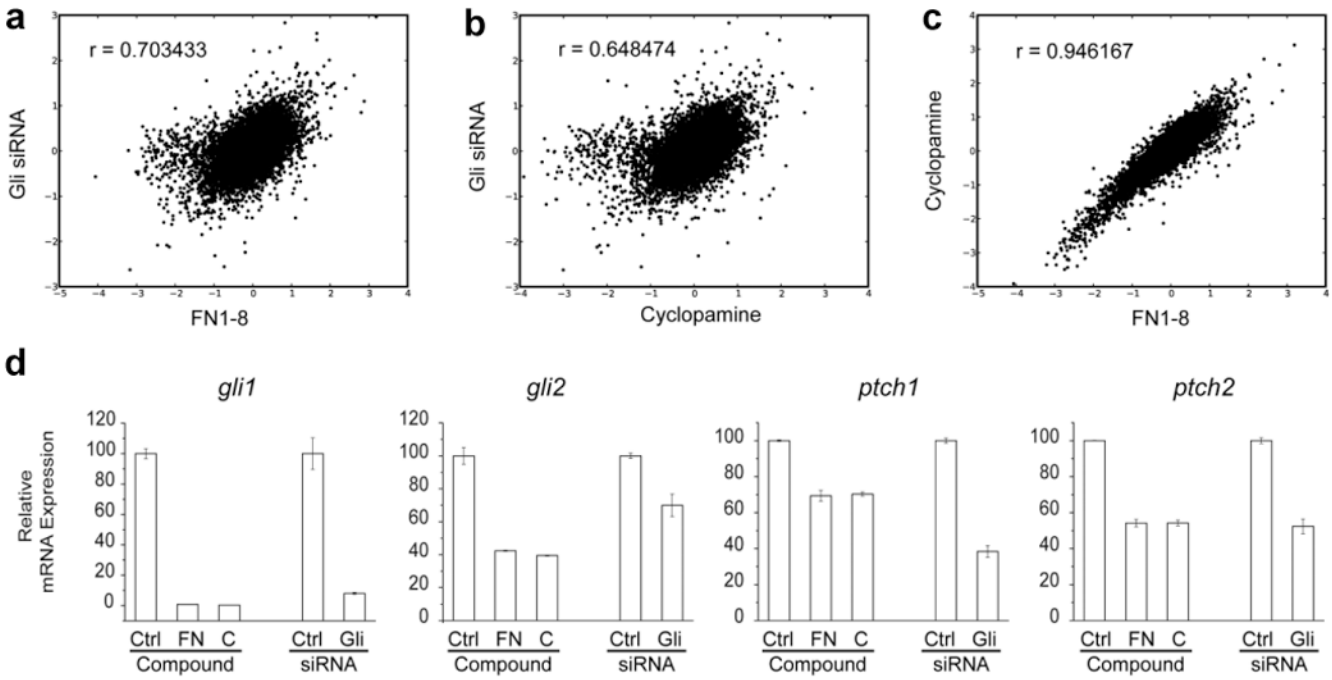

Figure 6.

Comparison of gene expressions in lung cancer cells treated with small molecule FN1-8, Gli siRNAs and cyclopamine. Microarray was used to examine global RNA expression profiles of H1299 cells treated with 10μM FN1-8, Gli siRNAs and 10μM cyclopamine. Correlation of changes in the gene expressions was analyzed in pairs: (a) FN1-8 treatment (x-axis) v.s. Gli siRNA treatment (y-axis); (b) cyclopamine treatment (x-axis) v.s. Gli siRNA treatment (y-axis); (c) FN1-8 treatment (x-axis) v.s. cyclopamine treatment (y-axis). p values of all r values <0.0001. (d) Quantitative real-time RT-PCR validation of the Hh effectors identified in microarray analyses. Y-axis represents relative mRNA expression (%). FN represents FN1-8, C represents cyclopamine. All the data represent means ± S.D.

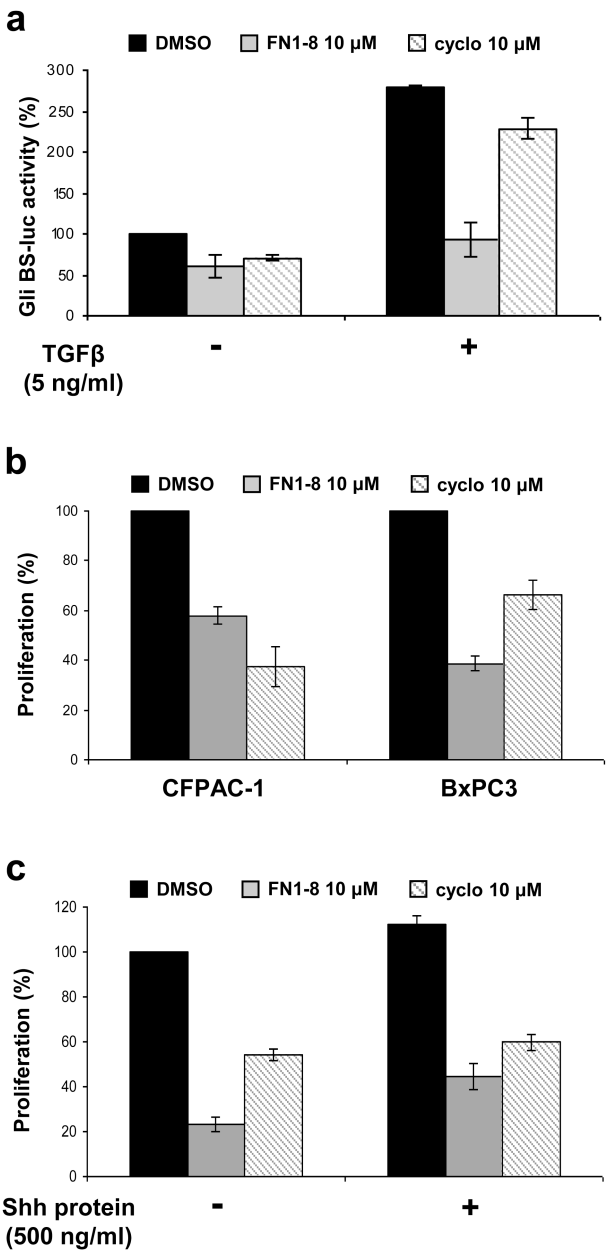

Figure 7.

Small molecule FN1-8 acts at the Gli level and downstream of Shh signaling. (**a**) FN1-8 inhibits TGFβ (5ng/ml) induced Gli-dependent transcriptional activity in A549 cells. All the measured luciferase activities were normalized to pRL-TK Vector activity. Cyclo represents cyclopamine. (**b**) Proliferation assay of pancreatic cell lines BXPC3 lacking SMO expression and CFPAC over-expressing SMO after FN1-8 and cyclopamine treatment (10µM). (**c**) Proliferation assay of melanoma cell line LOX lacking Shh expression after FN1-8 and cyclopamine treatment (10µM) in the presence or absence of recombinant Shh protein (500ng/ml). All the data represent means ± S.D.

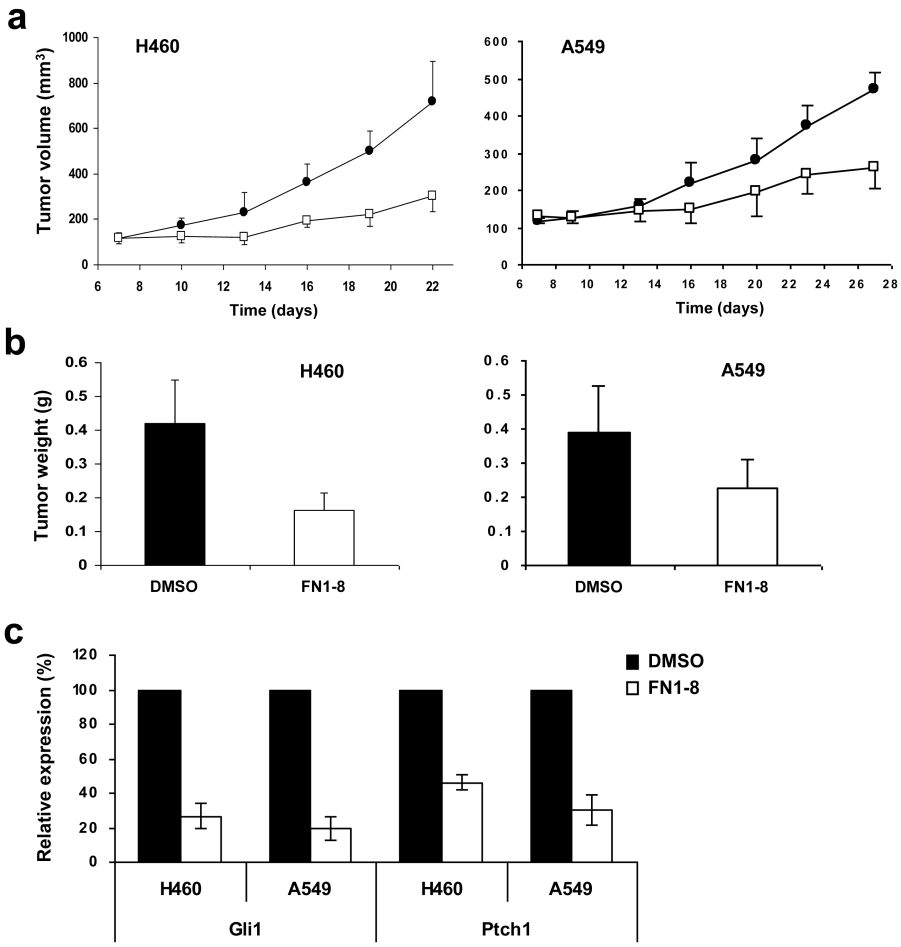

Figure 8.

Small molecule FN1-8 suppresses growth of lung cancer xenograft models in vivo. (**a**) Treatment with FN1-8 (50mg/kg body weight) or vehicle control started at day 7 after tumor inoculation and lasted for 12 days. Tumor size was measured every 3-4 days. Tumor volume was calculated by using the equation x^2y (where x<y). (**b**) Tumor weight at the completion of the experiment. (**c**) Real-time RT-PCR analysis of target genes of the Gli transcription. GAPDH was used as an internal control for normalization. All the data represent means ± S.D.